Journal of Hazardous Materials 192 (2011) 1192–1202

Contents lists available at ScienceDirect

Journal of Hazardous Materials

journal homepage: www.elsevier.com/locate/jhazmat

Structure elucidation and toxicity analyses of the radiolytic products of aflatoxin B_1 in methanol–water solution

Feng Wang[a,b,c], Fang Xie[a,b], Xiaofeng Xue[d], Zhidong Wang[a,b], Bei Fan[a,b], Yiming Ha[a,b,*]

[a] Institute of Agro-food Science and Technology of Chinese Academy of Agricultural Sciences, 2nd Yuanmingyuan West Road, Hai Dian District, Beijing 100193, PR China
[b] Key Opening Laboratory of Agricultural Products Processing and Quality Control, Ministry of Agriculture, 2nd Yuanmingyuan West Road, Hai Dian District, Beijing 100193, PR China
[c] Graduate School of Chinese Academy of Agricultural Sciences, 12th Zhongguancun South Road, Hai Dian District, Beijing 100081, PR China
[d] Bee Research Institute of Chinese Academy of Agricultural Sciences, 1st Xiangshan North Ditch, Hai Dian District, Beijing 100093, PR China

ARTICLE INFO

Article history:
Received 3 March 2011
Received in revised form 9 June 2011
Accepted 9 June 2011
Available online 17 June 2011

Keywords:
Aflatoxin B_1
Radiolytic products
LC–Q-TOF MS
Structure
Toxicity

ABSTRACT

The identification of the radiolytic products of mycotoxins is a key issue in the feasibility study of gamma ray radiation detoxification. Methanol–water solution (60:40, v/v) spiked with aflatoxin B_1 (AFB_1; 20 mg L^{-1}) was irradiated with Co^{60} gamma ray to generate radiolytic products. Liquid chromatography–quadruple time-of-flight mass spectrometry was applied to identify the radiolytic products of AFB_1. Accurate mass and proposed molecular formulas with a high-matching property of more than 20 radiolytic products were obtained. Seven key radiolytic products were proposed based on the molecular formulas and tandem mass spectrometry spectra. The analyses of toxicity and formation pathways were proposed based on the structure of the radiolytic products. The addition reaction caused by the free-radical species in the methanol–water solution resulted in the formation of most radiolytic products. Based on the structure–activity relationship analysis, the toxicity of radiolytic products was significantly reduced compared with that of AFB_1 because of the addition reaction that occurred on the double bond in the terminal furan ring. For this reason, gamma irradiation is deemed an effective tool for the detoxification of AFB_1.

1. Introduction

Aflatoxins, the secondary metabolites of *Aspergillus flavus* and *Aspergillus parasiticus*, are highly toxic, mutagenic, and carcinogenic compounds implicated as causative agents in human hepatic and extrahepatic carcinogenesis [1,2]. Among a variety of aflatoxin species, aflatoxin B_1 (AFB_1) is the most potent teratogen, mutagen, and hepatocarcinogen, and is classified as a group 1 carcinogen by the International Agency for Research in Cancer [3]. Aflatoxins occur in many countries, especially in tropical and subtropical regions where the conditions of temperature and humidity are optimal for the growth of moulds and for the production of the toxin. Many agricultural commodities and important crops, such as peanuts and peanut-based foods, are susceptible to such contamination [4,5].

The removal of aflatoxins from agricultural products is an area of research interest and government concern [6–12]. The γ-irradiation of AFB_1 was reported to have encouraging degradation rates in several studies [13–16]. However, both the identification of radiolytic products and the confirmation of toxicity have been poorly studied.

In our previous work, liquid chromatography–tandem mass spectrometry (LC–MS/MS) revealed that the number of radiolytic products in solution is large and that the concentration of every product is very low [16,17]. These limitations make the structure elucidation of all radiolytic products difficult and challenging. The use of analytical methods that are not only sensitive and good at separation, but also capable of dealing with enough qualitative information is required to support the recognition and structural elucidation of "unknown" compounds that could be present. Mass measurement and multiple stages of mass spectrometry can be jointed in quadruple time-of-flight mass spectrometry (Q-TOF MS). For this reason, high-performance LC–Q-TOF MS (HPLC–Q-TOF MS) was chosen to identify the radiolytic products of AFB_1 in this study. Accurate mass measurements from TOF generate the elemental compositions of ions (molecules and fragments). Moreover, MS^2 provide complementary structural information through in-source fragmentation using collision-induced dissociation (CID). Pico [18] reviewed the application of Q-TOF MS in analyzing metabolites and degradation products of food contaminants. This method was proved to be qualified for the elucidation of unknown compounds at trace levels in complex food extracts [19–24]. Liu (2010) iden-

* Corresponding author at: Institute of Agro-food Science and Technology of Chinese Academy of Agricultural Sciences, 2nd Yuanmingyuan West Road, Hai Dian District, Beijing 100193, PR China. Tel.: +86 10 6281 5969; fax: +86 10 6282 9727.
E-mail address: wxfay2011@hotmail.com (Y. Ha).

0304-3894/$ – see front matter © 2011 Elsevier B.V. All rights reserved.
doi:10.1016/j.jhazmat.2011.06.027

tified three major photo-degradation products resulting from the ultraviolet irradiation of AFB_1 using ultra-performance LC–Q-TOF; the results of the aforementioned study gave us more confidence in using Q-TOF MS in our experiment [25,26].

The purpose of the present study was to apply the accurate mass measurements of both precursor and product ions collected using HPLC–Q-TOF, and to combine Q-TOF MS and Q-TOF MS/MS spectrum to identify the γ-irradiation radiolytic products of AFB_1 in methanol–water solution (60:40, v/v). The identification of radiolytic products is important to the toxicity analysis of the γ-irradiation AFB_1 solution and for proposing an irradiation degradation route that should provide clues for understanding the food-safety aspects of γ-irradiation AFB_1 decontamination.

2. Experimental

2.1. Chemicals and reagents

AFB_1 (2,3,6a,9a-tetrahydro-4-methoxycyclopenta[c]furo [2,3:4,5]furo[2,3-h]chromene-1,11-dione; $C_{17}H_{12}O_6$; purity >98%) was obtained from Fermentek (Jerusalem, Israel). HPLC-grade methanol was purchased from Sigma (St. Louis, MO).

For the LC–Q-TOF MS studies, deionized water (18-MX cm^{-1} resistivity) was obtained from Milli-Q SP Reagent Water system (Millipore, Bedford, MA) and pre-filtered through a 0.2 μm filter.

Standard stock solutions (40 mg L^{-1}) of AFB_1 were prepared in methanol and stored at 4 ± 2 °C in a refrigerated dark room. A total of 0.5 mL of the standard stock solutions were placed in glass tubes and dried under a jet of nitrogen immediately before use. The working solution (20 mg L^{-1}) of AFB_1 was prepared by adding 1 mL of methanol–water solution (60:40, v/v).

2.2. Gamma irradiation

For radiolytic experiments, the solutions (20 mg L^{-1}) of pure AFB_1 in sealed glass centrifuge tubes were irradiated at room temperature in doses of 0, 5, 7, and 10 kGy using ^{60}Co source (Chinese Agricultural Radiation Center). The average dose rate was 0.31 Gy s^{-1}. Sunlight was avoided using foil throughout the irradiation process. The experiment was performed in triplicate for each sample.

2.3. LC–Q-TOF MS operating conditions

LC was performed on an Agilent 1100 Series HPLC (Agilent, Palo Alto, CA) equipped with an auto-injector, quaternary HPLC pump. Chromatography was performed on a 2.1 mm × 150 mm 5 μm Agilent extent C_{18} column. The injection volume was 5 μL. The mobile phase was methanol (component A) and an aqueous solution containing 0.1% formic acid (component B) in 60:40 (v/v) solution. Total run time was 8 min, with flow rate of 0.3 mL min^{-1}.

MS was performed with an Agilent 6510 ESI Q-TOF. The optimized conditions were as follows: MS source parameters were set with a capillary voltage of 3.5 kV in positive ionization mode. The fragmentor voltage was 150 V, and the skimmer was 65 V. The gas temperature was 350 °C, drying gas was 9 L/min, and nebulizer was 45 psi. Nitrogen was used as collision gas. MS spectra were acquired in a full scan analysis within the range of 100–1000 *m/z* using an extended dynamic range and a scan rate of 1.4 spectra/s, and by varying collision energy with mass. The data station operating software used was the Mass Hunter Workstation software (Version B.01.03). A reference mass solution containing reference ions 121.0508 and 922.0097 was used to maintain mass accuracy during the run time.

2.4. Data analysis

When spiked into the HPLC–Q-TOF MS, the sample components were made to go through the separation column into the MS ion source to ionise, and then through the first quadruple to reach the time of flight mass analyzer without CID. The background noise and the irrelevant ions were excluded from the results using molecular feature extraction (MFE) data files, a function of the Mass Hunter Workstation software. Subsequently, all possible components were

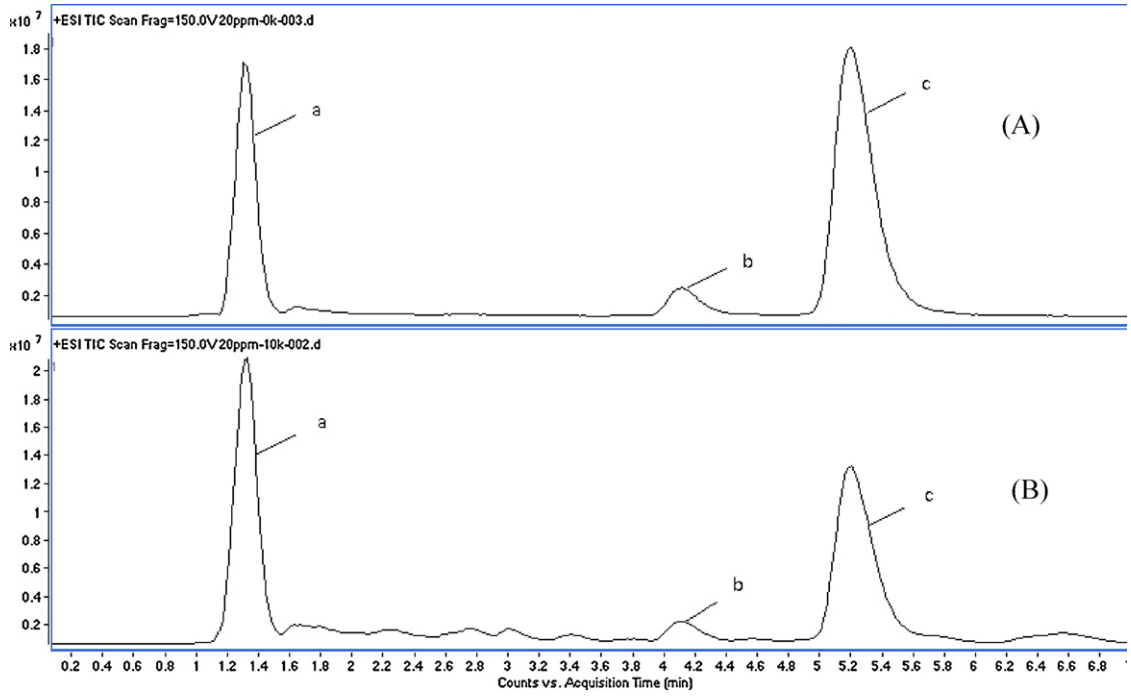

Fig. 1. LC–Q-TOF MS total ion chromatograms corresponding to (A) AFB_1 in the methanol–water solution before gamma irradiation and (B) AFB_1 and radiolytic products in the methanol–water solution after 10 kGy gamma irradiation. Peak a, solvent peak; peak b, AFB_2 as impurity; peak c, AFB_1, initial concentration 20 mg L^{-1}.

Table 1
Mass accuracy measurement of AFB_1[a] radiolytic products[b] using HPLC–Q-TOF MS.

Retention time (min)	Experimental mass[c] (*m/z*)	Theoretical mass[c] (*m/z*)	Elemental composition	Error		DBE	Scores
				mDa	ppm		
1.847	363.0715	363.0711	$C_{17}H_{14}O_9$	0.4	1.1	11	82.49
1.926	305.0654	305.0656	$C_{15}H_{12}O_7$	−0.2	−0.7	10	98.7
1.857	347.0762	347.0761	$C_{17}H_{14}O_8$*	0.1	0.3	11	94.05
1.985	363.0724	363.0711	$C_{17}H_{14}O_9$	1.3	3.6	11	73.7
2.025	377.0869	377.0867	$C_{18}H_{16}O_9$	0.2	0.5	11	73
2.261	347.0766	347.0761	$C_{17}H_{14}O_8$*	0.5	1.4	11	96.28
2.330	319.0813	319.0812	$C_{16}H_{14}O_7$*	0.1	0.3	10	98.36
2.408	331.0818	331.0812	$C_{17}H_{14}O_7$*	0.6	1.8	11	98.48
2.910	361.0922	361.0918	$C_{18}H_{16}O_8$*	0.4	1.1	11	93.25
2.910	725.1482	725.1501	$C_{38}H_{28}O_{15}$	−1.9	−2.6	25	92.48
3.077	343.0818	343.0812	$C_{18}H_{14}O_7$	0.6	1.7	12	46.48
3.077	317.0665	317.0656	$C_{16}H_{12}O_7$	0.9	2.8	11	82.08
3.215	329.0660	329.0656	$C_{17}H_{12}O_7$	0.4	1.2	10	97.7
3.411	363.1077	363.1074	$C_{18}H_{18}O_8$	0.3	0.8	10	81.07
3.579	275.0560	275.055	$C_{14}H_{10}O_6$*	1	3.6	10	80.92
3.618	331.0821	331.0812	$C_{17}H_{14}O_7$	0.9	2.7	11	80.61
3.550	327.0869	327.0863	$C_{18}H_{14}O_6$	0.6	1.8	12	83.72
3.904	347.0763	347.0761	$C_{17}H_{14}O_8$	0.2	0.6	11	84.41
3.983	379.1034	379.1024	$C_{18}H_{18}O_9$	1	2.6	10	80.24
4.032	283.0610	283.0601	$C_{16}H_{10}O_5$*	0.9	3.2	12	82.81
4.022	305.0642	305.0656	$C_{15}H_{12}O_7$	−1.4	−4.6	10	73.91
4.534	329.0660	329.0656	$C_{17}H_{12}O_7$	0.4	1.2	12	96.41
6.551	297.0762	297.0757	$C_{17}H_{12}O_5$	0.5	1.7	12	83.81
6.846	327.0871	327.0863	$C_{18}H_{14}O_6$	0.8	2.4	12	80.41
5.744 AFB_1	313.0711	313.0707	$C_{17}H_{12}O_6$	0.4	1.3	12	97.77

[a] AFB_1 initial concentration: 20 mg L^{-1}.
[b] γ-Irradiation dose: 10 kGy.
[c] All the *m/z* in our experiment is the *m/z* of $[M+H]^+$ (ionized mass with the less of an electron than the neutral mass M+H).

calculated and listed. Accurate masses were obtained using Agilent 6510 Q-TOF with a mass error less than 5 ppm, which allowed us to generate one or a few possible formulas quickly. In addition, the isotopic distribution was further confirmed. The formulas of possible components were obtained using molecular formula generation (MFG), another function of the Mass Hunter Workstation software.

The CID mode was used for further analysis. The retention time and the parent ion of each target analyte were input in the method, and after the method setting was completed, the sample was spiked for the second time for MS/MS analysis. The parent ions were fragmented, and the fragmentation pathways were obtained. The MFGs were also used for calculating the formula of fragment ions with accurate mass. The final identification of an unknown compound was then performed based on the accurate measurement of the mass of the parent ions and the fragments, as well as other useful MS/MS spectrum information.

3. Results and discussion

3.1. Identification of AFB_1 radiolytic products using LC–Q-TOF MS

3.1.1. Molecular formulas of radiolytic products

Fig. 1 shows the typical Q-TOF MS total ion chromatograms (scan range from 100 to 1000 *m/z*) of the samples before (Fig. 1A) and after the γ-irradiation (Fig. 1B; irradiation dose, 10 kGy; AFB_1 initial concentration, 20 mg L^{-1}). Based on the comparison of Fig. 1A with B, many other peaks in Fig. 1B showing the emergence of the radiolytic products were found in addition to AFB_1, AFB_2 (impurity), and solvent peaks. However, compared with the AFB_1 peak, the radiolytic product peaks were very small in the total ion chromatogram. For this reason, any peak that can be calculated using the molecular formulae is listed in Table 1. The table lists the retention time, the exact masses, the possible empirical formula, the mass error (ppm), the double bond equivalent (DBE), and the scores of radiolytic products obtained using Q-TOF MS. For all the products, the empirical formula (assigned with errors of <5 ppm) was coherent with their tentative identification, which was a good preliminary confirmation of the identity of the products. The score is a compositive index rated on a scale of 100 (an index closer to 100 is better) that includes both the mass calculated from the formulas and the isotope pattern match. However, some isotope information was weak because AFB_1 and its radiolytic products contained only three elements (i.e., carbon, hydrogen, and oxygen). In addition, the responses of radiolytic products in the Q-TOF were also very weak because some radiolytic products had very low concentrations; hence, many scores shown in Table 1 are not high.

In irradiation chemistry, the radiolytic process is influenced by many factors, such as absorbed doses, initial AFB_1 concentration, and position in the irradiation system [13,27,28]. Thus, given that radiolytic products are subject to these factors, the products were not exactly the same. To understand this effect better, a radiolytic product that can be detected after 10 kGy irradiation but could not be detected after 5 kGy irradiation is assumed; the latter production may be too low to reach the instrument detection limit. However, no matter how the influence factors changed in different experiments, seven key products marked with "*" were still found

Table 2
Validation of the retention time reproducibility[a] of the seven key radiolytic products.

Elemental composition	Theoretical mass (*m/z*)	Retention time (min)	RSD[b] (%)
$C_{17}H_{14}O_8$*	347.0761	1.850 ± 0.008	0.43
$C_{17}H_{14}O_8$*	347.0761	2.259 ± 0.007	0.31
$C_{16}H_{14}O_7$*	319.0812	2.331 ± 0.008	0.34
$C_{17}H_{14}O_7$*	331.0812	2.410 ± 0.008	0.32
$C_{18}H_{16}O_8$*	361.0918	2.908 ± 0.016	0.55
$C_{14}H_{10}O_6$*	275.055	3.570 ± 0.036	1.01
$C_{16}H_{10}O_5$*	283.0601	4.036 ± 0.039	0.97

[a] $n = 9$; 3 replicates were treated at irradiation doses of 5, 7, and 10 kGy; AFB_1 initial concentration: 20 mg L^{-1}.
[b] RSD: relative standard deviation.

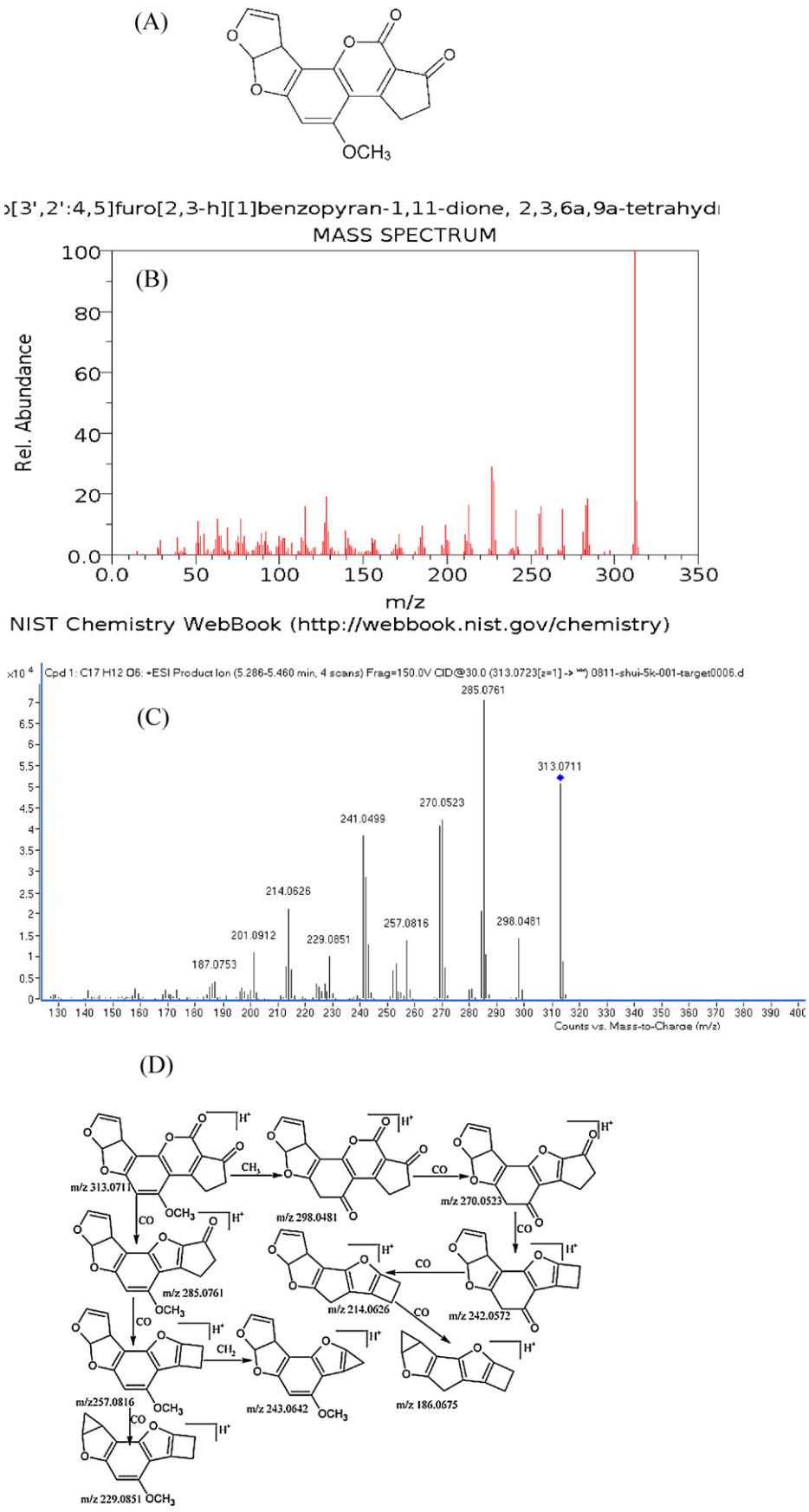

Fig. 2. (A) The structure of AFB_1; (B) the MS/MS spectrum of AFB_1, obtained from the NIST Mass Spec Data Center; (C) HPLC–Q-TOF MS/MS spectrum of AFB_1; (D) fragmentation pathway of AFB_1.

Table 3
Accurate mass measurements of the product ions of AFB_1 and its seven key radiolytic products using HPLC–Q-TOF in the MS/MS mode.

Retention time (min)	Mass (*m*/*z*)	Formula	Abund (%)	Diff (ppm)	Loss mass	Loss formula	[a]CE (eV)
5.744	313.0711	$C_{17}H_{13}O_6$					30
AFB_1	298.0484	$C_{16}H_{10}O_6$	3.65	−2.96	15.0235	CH_3	
	285.0761	$C_{16}H_{13}O_5$	20.93	−1.1	27.9949	CO	
	284.0687	$C_{16}H_{12}O_5$	5.3	−7.89	29.0027	CHO	
	270.0523	$C_{15}H_{10}O_5$	12.86	−0.02	43.0184	C_2H_3O	
	269.0451	$C_{15}H_9O_5$	10.54	−2.59	44.0262	C_2H_4O	
	257.0816	$C_{15}H_{13}O_4$	3.56	−3.03	55.9898	C_2O_2	
	253.0493	$C_{15}H_9O_4$	2.18	0.83	60.0211	$C_2H_4O_2$	
	252.0421	$C_{15}H_8O_4$	1.77	−1.31	61.0290	$C_2H_5O_2$	
	243.0642	$C_{14}H_{11}O_4$	3.32	4.17	70.0055	$C_3H_2O_2$	
	242.0572	$C_{14}H_{10}O_4$	7.43	0.66	71.0133	$C_3H_3O_2$	
	241.0499	$C_{14}H_9O_4$	9.92	−1.64	72.0211	$C_3H_4O_2$	
	229.0851	$C_{14}H_{13}O_3$	2.58	3.5	83.9847	C_3O_3	
	227.0355	$C_{13}H_7O_4$	0.94	−6.97	86.0368	$C_4H_6O_2$	
	224.0477	$C_{14}H_8O_3$	0.91	−4.05	89.0239	$C_3H_5O_3$	
	214.0626	$C_{13}H_{10}O_3$	7.29	−0.58	99.0082	$C_4H_3O_3$	
	213.055	$C_{13}H_9O_3$	2	−1.77	100.016	$C_4H_4O_3$	
	201.0912	$C_{13}H_{13}O_2$	2.84	−1.12	111.9797	C_4O_4	
	187.0753	$C_{12}H_{11}O_2$	1.02	0.26	125.9953	$C_5H_2O_4$	
	186.0675		0.94				
1.857	347.0762	$C_{17}H_{14}O_8$					25
	329.0623	$C_{17}H_{13}O_7$	10.68	9.99	18.0106	H_2O	
	315.0482	$C_{16}H_{11}O_7$	1.49	5.63	32.0262	CH_4O	
	311.0519	$C_{17}H_{11}O_6$	1.56	9.88	36.0211	H_4O_2	
	301.0674	$C_{16}H_{13}O_6$	16.68	10.99	46.0055	CH_2O_2	
	289.068	$C_{15}H_{13}O_6$	4.35	9.21	58.0055	$C_2H_2O_2$	
	287.0517	$C_{15}H_{11}O_6$	4.65	11.71	60.0211	$C_2H_4O_2$	
	283.0577	$C_{16}H_{11}O_5$	12.3	8.37	64.016	CH_4O_3	
	273.0737	$C_{15}H_{13}O_5$	32.22	7.33	74.0004	$C_2H_2O_3$	
	259.0575	$C_{14}H_{11}O_5$	4.75	9.85	88.016	$C_3H_4O_3$	
	258.0509	$C_{14}H_{10}O_5$	2.02	3.18	89.0239	$C_3H_5O_3$	
	257.0697	$C_{11}H_{13}O_7$	2.51	−15.84	90.0106	C_6H_2O	
	255.0633	$C_{15}H_{11}O_4$	3.39	7.31	92.011	$C_2H_4O_4$	
	229.0469	$C_{13}H_9O_4$	1.69	11.72	118.0266	$C_4H_6O_4$	
	227.0685	$C_{14}H_{11}O_3$	1.7	7.79	120.0059	$C_3H_4O_5$	
2.261	347.0766	$C_{17}H_{14}O_8$					25
	317.0653	$C_{16}H_{13}O_7$	15.36	0.73	30.0106	CH_2O	
	301.0683	$C_{16}H_{13}O_6$	3.14	8.02	46.0055	CH_2O_2	
	299.0529	$C_{16}H_{11}O_6$	3.43	6.95	48.0211	CH_4O_2	
	289.0706	$C_{15}H_{13}O_6$	30.46	0.35	58.0055	$C_2H_2O_2$	
	273.0793	$C_{15}H_{13}O_5$	2.33	−12.9	74.0004	$C_2H_2O_3$	
	271.0601	$C_{15}H_{11}O_5$	3.98	0.11	76.016	$C_2H_4O_3$	
	261.0758	$C_{14}H_{13}O_5$	3.19	−0.3	86.0004	$C_3H_2O_3$	
	259.0584	$C_{14}H_{11}O_5$	1.99	6.72	88.016	$C_3H_4O_3$	
	245.0448	$C_{13}H_9O_5$	14.99	−1.33	102.0317	$C_4H_6O_3$	
2.330	319.0813	$C_{16}H_{14}O_7$					25
	301.068	$C_{16}H_{13}O_6$	20.17	8.71	18.0106	H_2O	
	273.0738	$C_{15}H_{13}O_5$	44.53	7.09	46.0055	CH_2O_2	
	259.0572	$C_{14}H_{11}O_5$	15.58	11.02	60.0211	$C_2H_4O_2$	
	258.0473	$C_{14}H_{10}O_5$	1.84	11.33	61.0290	$C_2H_5O_2$	
	247.0576	$C_{13}H_{11}O_5$	3.15	10.11	72.0211	$C_3H_4O_2$	
	245.0765	$C_{14}H_{13}O_4$	4.29	17.71	74.0004	$C_2H_2O_3$	
	229.048	$C_{13}H_9O_4$	2.27	6.54	90.0317	$C_3H_6O_3$	
	217.0828	$C_{13}H_{13}O_3$	3.43	14.38	101.9953	$C_3H_2O_4$	
	203.0696	$C_{12}H_{11}O_3$	4.73	3.2	116.011	$C_4H_4O_4$	
2.408	331.0821	$C_{17}H_{14}O_7$					25
	313.0681	$C_{17}H_{13}O_6$	36.91	8.13	18.0106	H_2O	
	298.0454	$C_{16}H_{10}O_6$	2.44	−4.82	33.034	CH_5O	
	285.0728	$C_{16}H_{13}O_5$	24.41	10.43	46.0055	CH_2O_2	
	284.0644	$C_{16}H_{12}O_5$	5.76	0.27	47.0133	CH_3O_2	
	273.0743	$C_{15}H_{13}O_5$	4.28	5.29	58.0055	$C_2H_2O_2$	
	270.0497	$C_{15}H_{10}O_5$	7.04	−6.79	61.0290	$C_2H_5O_2$	
	269.0413	$C_{15}H_9O_5$	3.16	11.63	62.0368	$C_2H_6O_2$	
	259.0597	$C_{14}H_{11}O_5$	2.06	1.67	72.0211	$C_3H_4O_2$	
	257.0795	$C_{15}H_{13}O_4$	3.64	5.04	74.0004	$C_2H_2O_3$	
	243.0613	$C_{14}H_{11}O_4$	2.72	15.87	88.016	$C_3H_4O_3$	
	242.0553	$C_{14}H_{10}O_4$	2.3	9.48	89.0239	$C_3H_5O_3$	
	241.0468	$C_{14}H_9O_4$	2.26	11.47	90.0317	$C_3H_6O_3$	
	229.0829	$C_{14}H_{13}O_3$	3.03	13.25	101.9953	$C_3H_2O_4$	
2.910	361.0922	$C_{18}H_{16}O_8$					25
	329.0623	$C_{17}H_{13}O_7$	15.06	9.92	32.0262	CH_4O	
	311.0525	$C_{17}H_{11}O_6$	2.98	7.97	50.0368	CH_6O_2	
	301.0768	$C_{16}H_{13}O_6$	20.67	9.45	60.0211	$C_2H_4O_2$	

Table 3 (*Continued*)

Retention time (min)	Mass (*m*/*z*)	Formula	Abund (%)	Diff (ppm)	Loss mass	Loss formula	[a]CE (eV)
	283.058	$C_{16}H_{11}O_5$	42.11	7.58	78.0317	$C_2H_6O_3$	
	273.074	$C_{15}H_{13}O_5$	6.58	6.48	88.016	$C_3H_4O_3$	
	259.0575	$C_{14}H_{11}O_5$	3.64	10.08	102.0317	$C_4H_6O_3$	
	255.0634	$C_{15}H_{11}O_4$	6.63	7.08	106.0266	$C_3H_6O_4$	
	227.068	$C_{14}H_{11}O_3$	2.34	9.96	134.0215	$C_4H_6O_5$	
3.579	275.0560	$C_{14}H_{10}O_6$					25
	273.0376	$C_{14}H_9O_6$	3.04	6.34	2.0157	H_2	
	247.0576	$C_{13}H_{11}O_5$	35.94	9.94	27.9949	CO	
	219.0632	$C_{12}H_{11}O_4$	52.13	8.92	55.9898	C_2O_2	
	205.0452	$C_{11}H_9O_4$	2.55	20.93	70.0055	$C_3H_2O_2$	
	204.0383	$C_{11}H_8O_4$	3.9	16.67	71.0133	$C_3H_3O_2$	
	163.0755	$C_{10}H_{11}O_2$	2.45	−1.08	111.9797	C_4O_4	
4.032	283.0610	$C_{16}H_{11}O_5$					20
	255.0631	$C_{15}H_{11}O_4$	69.47	8.03	27.9949	CO	
	254.0576	$C_{15}H_{10}O_4$	12.85	−1.1	29.0027	CHO	
	227.0713	$C_{14}H_{11}O_3$	7.68	−4.59	55.9898	C_2O_2	
	199.0737	$C_{13}H_{11}O_2$	10	8.41	83.9847	C_3O_3	

[a] CE: collision energy.

in all experiments ($n = 9$; 3 replicates were treated at irradiation doses of 5, 7, and 10 kGy; initial AFB_1 concentration, 20 mg L^{-1}). In this regard, the identification of these key radiolytic products was deemed more important. The validation of the retention time reproducibility of these key radiolytic products in different experiments is listed in Table 2.

3.1.2. Structural formulas of radiolytic products

Accurate *m*/*z* values did not confirm unequivocally the identity of the products; hence, further study on the fragmentation patterns and the accurate mass of the product ions is needed.

Accurate mass measurements were performed in the process of selecting the protonated molecules as precursor ions for MS/MS

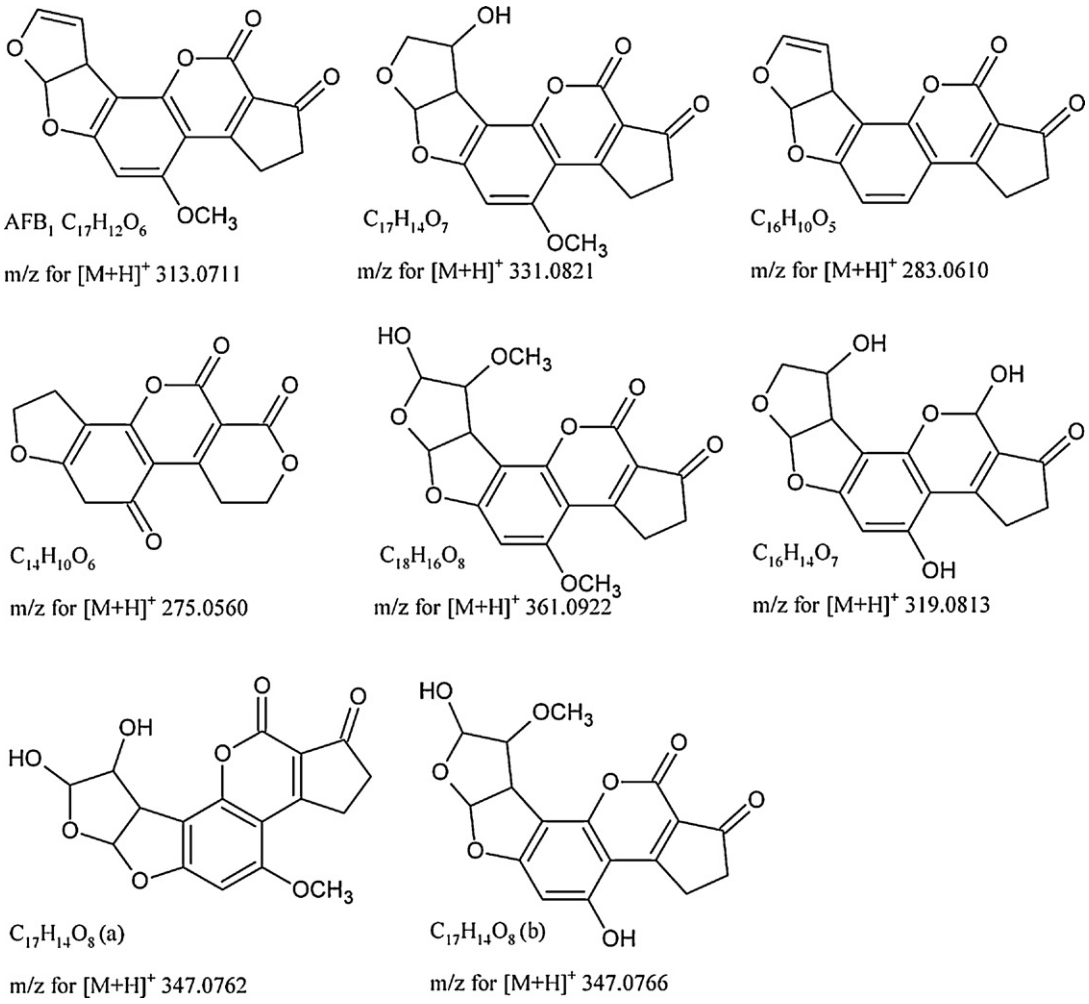

Fig. 3. Structures of AFB_1 and the seven key radiolytic products.

experiments to identify the radiolytic products. The results of these analyses along with the calculated values of the postulated ion masses of the radiolytic products and their fragment ions, as well as the mass error measured in parts per million for each compound, are listed in Table 3. Only the MS/MS spectrum of AFB_1 (Fig. 2C) was provided in this paper as an example to illustrate the analysis process. The MS/MS spectra of the radiolytic products were omitted because the available spectrum information is already listed in Table 3.

3.1.3. Analysis processes of radiolytic products

When methanol–water solution is irradiated, methanol, water, and AFB_1 absorb the radiation energy. The radiolysis of water yields reactive species called free radicals, such as hydroxyl (OH·), hydrated electrons (e_{aq}^-), and hydrogen atoms (H·); the radiolysis of methanol yields reactive methoxy species (OCH_3), and hydrogen atoms (H·) [29–31]. All radiolytic products are formed through the reaction of free radicals with AFB_1; therefore, their structures will be similar to that of AFB_1. The fragmentation pathway of AFB_1 has an important reference value in analyzing the fragmentation pathways of radiolytic products. The accurate mass measurements of product ions of AFB_1 are also listed in Table 3.

An electron ionization mass spectrum of AFB_1 obtained from the NIST Mass Spec Data Center was obtained to supply the supplementary information for the present analysis (Fig. 2B). Data obtained with both mass spectrometers (Q-TOF MS/MS and NIST Mass) were combined to establish the fragmentation pathway of AFB_1, as shown in Fig. 2D. The continuous loss of carbon monoxide

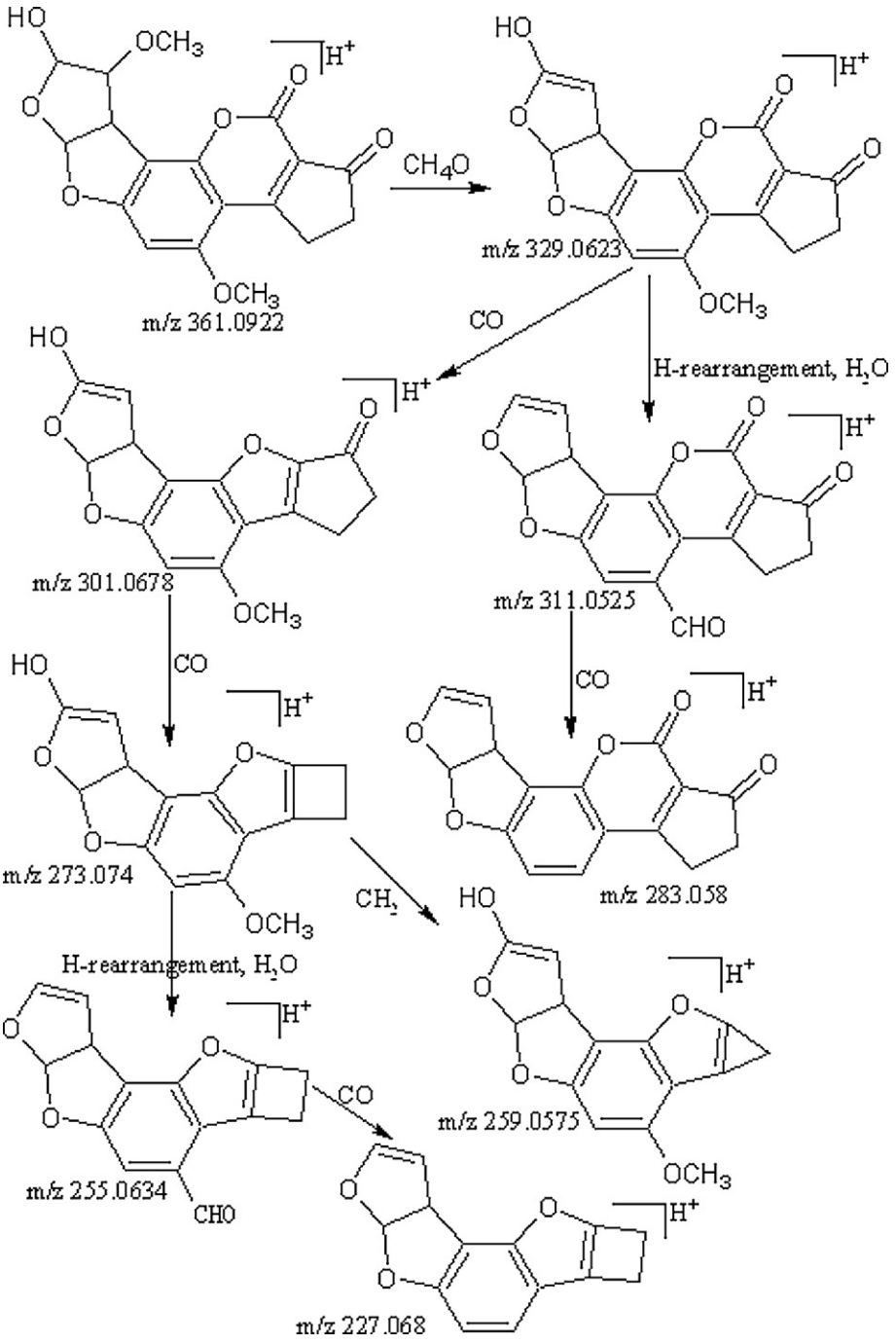

Fig. 4. Fragmentation pathway of the radiolytic product with 361.0922 *m/z*.

(CO) was the main fragmentation pathway. Methyl and methanol losses occurred on the methoxy group located on the side chain of benzene.

The radiolytic products were identified based on the accurate mass measurements of ions and similar fragmentation pathways with AFB_1.

The radiolytic product $C_{17}H_{14}O_7$ (with 331.0821 *m/z*) had one more H_2O molecule than AFB_1. The DBE of $C_{17}H_{14}O_7$ was 11, which was one less than AFB_1. When an H_2O molecule in the 331.0821 *m/z* was lost, the succeeding fragmentation pathway was the same as that of AFB_1. Therefore, the additional reaction of OH and H definitely occurred on the double bond of the furan ring on the left side. The radiolytic product $C_{16}H_{10}O_5$ (with 283.0610 *m/z*) had one less CH_2O molecule than AFB_1, and the DBE of $C_{16}H_{10}O_5$ was the same as that of AFB_1. The fragments reveal that the loss of CO was the main fragmentation pathway of 283.0610 *m/z*, which was the same as that of AFB_1. The structure was obtained by the loss of a methoxy group on the side chain of the benzene ring. The radiolytic product $C_{14}H_{10}O_6$ (with 275.0560 *m/z*) had less C_3H_2 molecules than AFB_1, whereas the DBE of $C_{14}H_{10}O_6$ was the same as that of AFB_1. The fragments also demonstrate that the loss of CO was the main fragmentation pathway of 275.0560 *m/z*, which was the same as that of AFB_1. Given that the fragmentation pathways of 331.0821, 283.0610, and 275.0560 *m/z* were similar with that of AFB_1, the figures of fragmentation pathways are not listed because of limitations in space; their structures are listed in Fig. 3.

The radiolytic product $C_{18}H_{16}O_8$ (with 361.0922 *m/z*) had more CH_4O_2 molecules than AFB_1, and $C_{18}H_{16}O_8$ had one less DBE than AFB_1, implying that an addition reaction occurred and that the fragments determined the position (the double bond of the furan ring on the left side). More details on the fragmentation pathway are shown in Fig. 4.

The radiolytic product $C_{16}H_{14}O_7$ (with 319.0813 *m/z*) had one less carbon atom, as well as had two more hydrogen atoms and one more oxygen atom than AFB_1. $C_{16}H_{14}O_7$ had one less DBE than AFB_1. Thus, by implication, an addition reaction occurred. The position was determined by the double bond located on the furan ring on the left side. In addition, the methoxy group on the side chain of the benzene ring was replaced by a hydroxyl group. More details on the fragmentation pathway are shown in Fig. 5.

The radiolytic product $C_{17}H_{14}O_8$ (with 347.0766 *m/z*) had more H_2O_2 molecules than AFB_1, whereas it had one less DBE than AFB_1. This result is most likely caused by an additional reaction of two hydroxyl groups on the double bond of the furan ring on the left side. The fragments show that the structure of $C_{17}H_{14}O_8$(a) in Fig. 1 was satisfied. More details on the fragmentation pathway are shown in Fig. 6.

The fragments of $C_{17}H_{14}O_8$(b) show losses of CH_2O and CH_2O_2. Therefore, the hydroxyl and the methoxy groups must be adjacent. A hydroxyl group could replace the methoxy group on the side chain of the benzene ring. The fragments show that the structure in Fig. 1 was satisfied. More details on the fragmentation pathway are shown in Fig. 7.

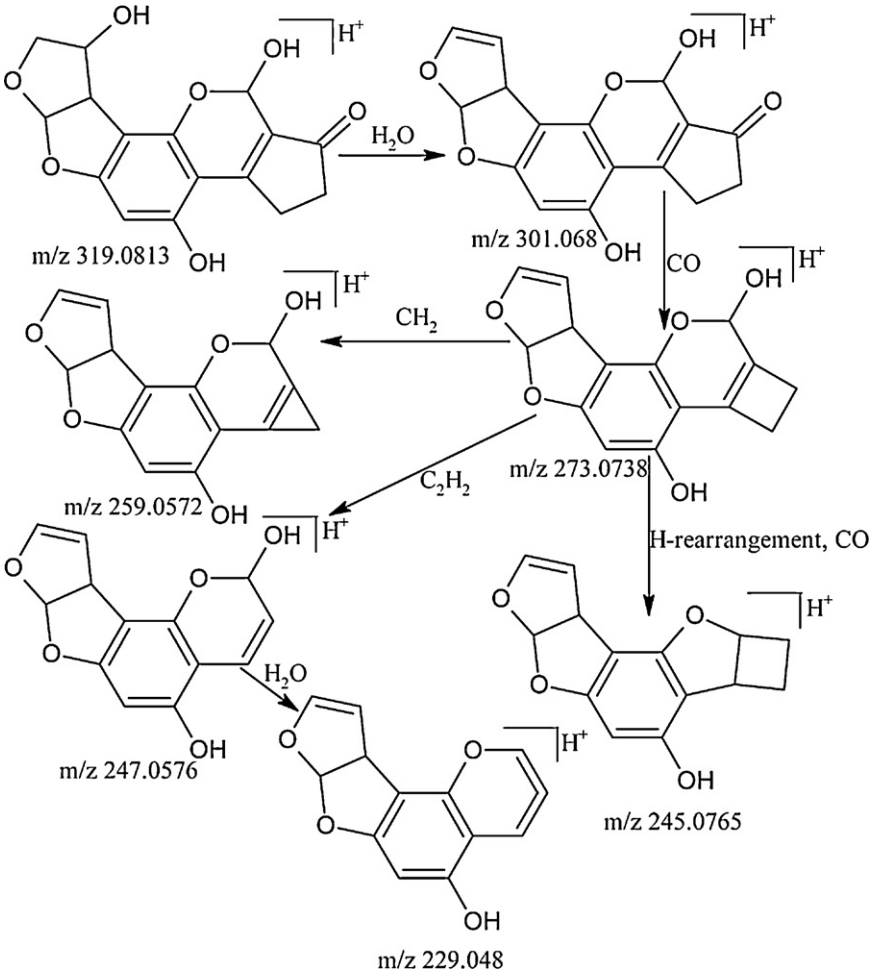

Fig. 5. Fragmentation pathway of the radiolytic product with 319.0813 *m/z*.

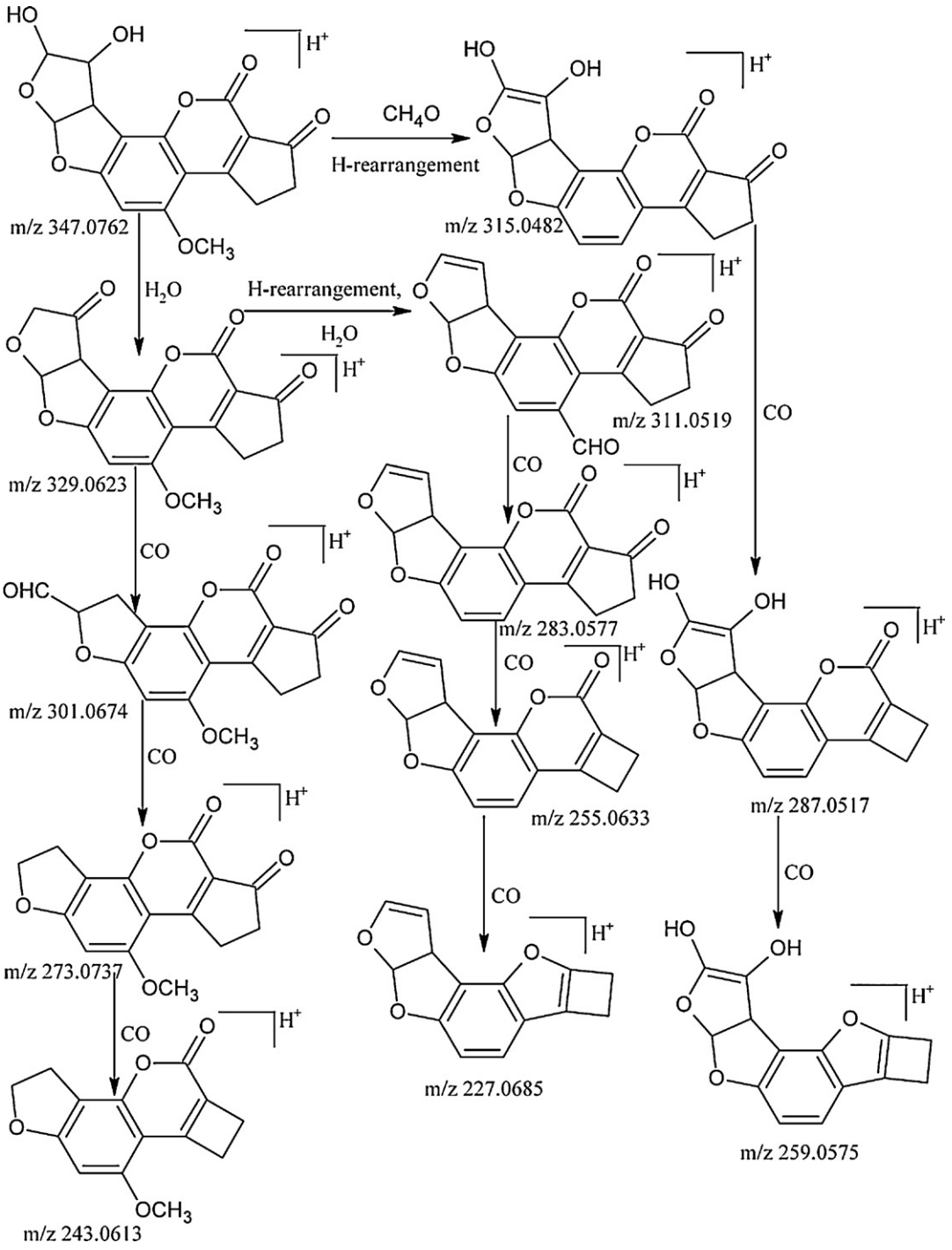

Fig. 6. Fragmentation pathway of the radiolytic product with 347.0762 *m/z*.

3.2. Toxicity analyses of radiolytic products based on the quantitative structure–activity relationship (QSAR)

Since the early 1960s, QSARs among aflatoxins have been deeply investigated by many research groups, such as Carnaghan, Wogan, and Bauer, among others. Similar conclusions have been reported with respect to aflatoxin toxicity to rainbow trout, zebra fish larvae, chicken embryos, ducklings, and rats, as well as to cultures of human embryonic lung and liver cells. These toxicity data suggested a structure–activity series with decreasing potency in the following order of aflatoxins: $B_1 > G_1 > B_2 > G_2$. The furofuran moiety of the aflatoxin structure is essential for toxic and carcinogenic activity. Moreover, the presence of the double bond in the terminal furan ring is an important determinant of potency, particularly for acute and chronic effects in rats [32–34].

In this study, based on the data collected using Q-TOF, DBE was a calculated indication of the number of double bonds and/or rings in the molecular structure. The DBE of AFB_1 was 12. Table 1 shows that a DBE of 70% of the radiolytic products were lower than that of AFB_1; some were 10 and the others were 11, implying that double bond addition reactions occurred. Based on the structures of the seven key radiolytic products shown in Fig. 3, the addition reaction

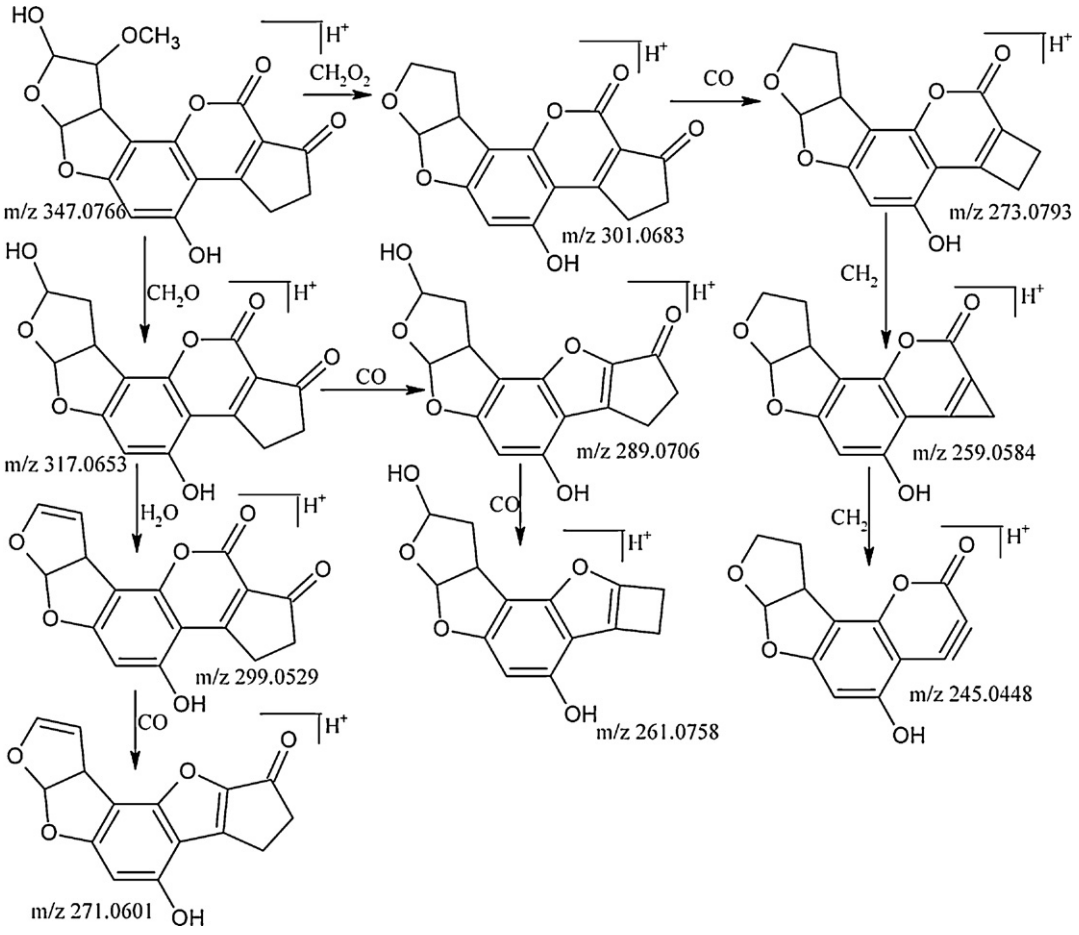

Fig. 7. Fragmentation pathway of the radiolytic product with 347.0766 *m/z*.

occurred on the double bond in the terminal furan ring. The double bond in the terminal furan ring is an important determinant of potency, particularly for acute and chronic effects in rats; however, this bond was no longer in existence in six of the seven key radiolytic products. Therefore, based on QSAR, the toxicity of total radiolytic products compared with that of AFB_1 was reduced.

Compared with animal or cytotoxicity experiments, toxicity analyses of radiolytic products based on QSAR is a back-of-envelope toxicological study. Nevertheless, this analysis is important. An ongoing study is conducted to detect AFB_1 radiolytic products in peanuts contaminated with high concentrations of AFB_1. If some of the radiolytic products reported in this paper are detected in the peanuts, 90 d animal experiments will be conducted using mice fed with peanuts contaminated by AFB_1 and radiolytic products.

3.3. Discussion

In actual food, the level of AFB_1 contamination is trace. The process of extraction and purification of radiolytic products is complex, and the structure elucidation of these products is very difficult. Therefore, water was selected as the medium in this study. When water is irradiated, free radicals are produced. The degradation of AFB_1 is performed virtually by these free radicals from the water. In addition, because AFB_1 is insoluble in water but soluble in methanol, a certain percentage of methanol was added in water to help the dissolution of AFB_1. The proportions of methanol and water were the same with the proportions in liquid chromatography mobile phase in order to eliminate the interference of solvent effect.

4. Conclusions

The radiolytic products of AFB_1 in methanol–water solution are complex in species and produce low concentrations of each product. In this study, LC–Q-TOF was proved to be the ideal tool for structure elucidation of unknown radiolytic products. Accurate mass measurements from TOF generate the elemental compositions of ions (molecules and fragments); tandem mass spectrometry spectra provide complementary structural information. The structures of seven key radiolytic products are listed in this paper. Based on the structures of the radiolytic products, free radical mechanisms are involved in the irradiation of AFB_1. The toxicity assessment of radiolytic products is also been proposed. Given that the addition reaction occurred with the formation of most radiolytic products, their toxicities were reduced compared with that of AFB_1.

Acknowledgements

This study was financially supported by the Special Fund for Agro-scientific Research in the Public Interest of PR China and the 948 project (No. 2010-G1) from the Ministry of Agriculture of China.

References

[1] HKSAR, Risk Assessment studies Report No.5: Chemical Hazards Evaluation, Hong Kong, 2001.
[2] J.L. Herrman, R. Walker, FAO/WHO Expert Committee on Food Additives (JECFA) in http://www.fao.org/docrep/x2100t/x2100t04.htm.
[3] IARC, Monograph on the evaluation of carcinogenic risk to humans. 80 (2002) 171. Organisation.

[4] W.O. Ellis, P. Smith, B.K. Simpson, Aflatoxins in food: occurrence, biosynthesis, effects on organisms, detection, and methods of control, Crit. Rev. Food Sci. Nutr. 30 (1991) 403–439.
[5] J.D. Miller, Fungi and mycotoxins in grain: Implications for stored product research, J. Stored Prod. Res. 30 (1994) 1–16.
[6] A. Méndez-Albores, G. Arámbula-Villa, M.G.F. Loarca-Piña, E. Castaño-Tostado, E. Moreno-Martínez, Safety and efficacy evaluation of aqueous citric acid to degrade B-aflatoxins in maize, Food Chem. Toxicol. 43 (2005) 233–238.
[7] A.D. Proctor, M. Ahmedna, J.V. Kumar, Degradation of aflatoxins in peanut kernels/flour by gaseous ozonation and mild heat treatment, Food Addit. Contam. B 21 (2004) 786–793.
[8] J.F. Alberts, Y. Engelbrecht, P.S. Steyn, Biological degradation of aflatoxin B_1 by *Rhodococcus erythropolis* cultures, Int. J. Food Microbiol. 109 (2006) 121–126.
[9] E. Kusumaningtyas, R. Widiastuti, R. Maryam, Reduction of aflatoxin B_1 in chicken feed by using *Saccharomyces cerevisiae*, *Rhizopus oligosporus* and their combination, Mycopathologia 162 (2006) 307–311.
[10] B.J. Park, K. Takatori, Y. Sugita-Konishi, Escherichia coli sterilization and lipopolysaccharide inactivation using microwave-induced argon plasma at atmospheric pressure, Surf. Coat. Tech. 201 (2007) 5733–5737.
[11] D. Guzmán-de-Peña, J.J. Peña-Cabriales, Regulatory considerations of aflatoxin contamination of food in Mexico, Rev. Latinoam. Microbiol. 47 (2005) 160–164.
[12] P. Sudhakar, P. Latha, Y. Sreenivasulu, Inhibition of *Aspergillus flavus* colonization and aflatoxin (AFB_1) in peanut by methyleugenol, Indian J. Exp. Biol. 47 (2009) 63–67.
[13] P.J. Van-Dyck, P. Tobback, M. Feys, H. van de Voorde, Sensitivity of aflatoxin B_1 to ionizing radiation, Appl. Environ. Microbiol. 43 (1982) 1317–1319.
[14] H. Hooshmand, C.F. Klopfenstein, Effects of gamma irradiation on mycotoxin disappearance and amino acid contents of corn, wheat, and soybeans with different moisture contents, Plant Foods Hum. Nutr. 47 (1995) 227–238.
[15] B.M. Youssef, S.R. Mahrous, N.H. Aziz, Effect of gamma irradiation on aflatoxin B_1 production by *Aspergillus flavus* in ground beef stored at 5 °C, J. Food Safety 19 (1999) 231–239.
[16] J. Yang, Y.M. Ha, Research on irradiation-induced degradation of mycotoxins in agricultural products, in: Chinese Academy of Agriculture Sciences Master Dissertation, Chinese Academy of Agriculture Sciences, Beijing, PR China, 2009.
[17] F. Xie, Y.M. Ha, F. Wang, Studies on Gamma irradiation induced degradation of chloramphenicol in aqueous solution, Chin. J. Radiat. Res. Radiat. Process 26 (2008) 151–156.
[18] Y. Pico, D. Barcelo, The expanding role of LC–MS in analyzing metabolites and degradation products of food contaminants, Trends Anal. Chem. 27 (2008) 821–835.
[19] Y. Pico, M. Farre, C. Soler, D. Barcelo, Confirmation of fenthion metabolites in oranges by IT-MS and QqTOF-MS, Anal. Chem. 79 (2007) 9350–9363.
[20] S. Lacorte, A.R. Fernandez-Alba, Time of flight mass spectrometry applied to the liquid chromatographic analysis of pesticides in water and food, Mass Spectrom. Rev. 25 (2006) 866–880.
[21] R. Rosal, M.S. Gonzalo, K. Boltes, P. Leton, J.J. Vaquero, E. Garcia-Calvo, Identification of intermediates and assessment of ecotoxicity in the oxidation products generated during the ozonation of clofibric acid, J. Hazard. Mater. 172 (2009) 1061–1068.
[22] E. Sobhanzadeh, N.K. Abu Bakar, M.R. Abas, K. Nemati, Low temperature followed by matrix solid-phase dispersion-sonication procedure for the determination of multiclass pesticides in palm oil using LC–TOF-MS, J. Hazard. Mater. 186 (2011) 1308–1313.
[23] A. Kaufmann, P. Butcher, K. Maden, Ultra-performance liquid chromatography coupled to time of flight mass spectrometry (UPLC–TOF): a novel tool for multiresidue screening of veterinary drugs in urine, Anal. Chim. Acta 586 (2007) 13–21.
[24] S. Grimalt, J.V. Sancho, O.J. Pozo, F. Hernandez, Quantification, confirmation and screening capability of UHPLC coupled to triple quadrupole and hybrid quadrupole time-of-flight mass spectrometry in pesticide residue analysis, J. Mass Spectrom. 45 (2010) 421–436.
[25] R.J. Liu, Q.Z. Jin, G.J. Tao, L. Shan, Y.F. Liu, X.G. Wang, LC–MS and UPLC–quadrupole time-of-flight MS for identification of photodegradation products of aflatoxin B_1, Chromatographia 71 (2010) 107–112.
[26] R.J. Liu, Q.Z. Jin, G.J. Tao, L. Shan, J.H. Huang, Y.F. Liu, X.G. Wang, Photodegradation kinetics and byproducts identification of the aflatoxin B_1 in aqueous medium by ultra-performance liquid chromatography–quadrupole time-of-flight mass spectrometry, J. Mass Spectrom. 45 (2010) 553–559.
[27] C. Slegers, B. Tilquin, Final product analysis in the e-beam and gamma radiolysis of aqueous solutions of metoprolol tartrate, Radiat. Phys. Chem. 75 (2006) 1006–1017.
[28] N. Getoff, Factors influencing the efficiency of radiation-induced degradation of water pollutants, Radiat. Phys. Chem. 65 (2002) 437–446.
[29] N. Getoff, Radiation-induced degradation of water pollutants—state of the art, Radiat. Phys. Chem. 47 (1996) 581–593.
[30] L. Huang, M. Zhai, J. Peng, J. Li, G. Wei, Radiation-induced degradation of carboxymethylated chitosan in aqueous solution, Carbohydr. Polym. 67 (2007) 305–312.
[31] M.A. Rauf, S.S. Ashraf, Radiation induced degradation of dyes—an overview, J. Hazard. Mater. 166 (2009) 6–16.
[32] G.N. Wogan, G.S. Edwards, P.M. Newberne, Structure–activity relationships in toxicity and carcinogenicity of aflatoxins and analogs, Cancer Res. 31 (1971) 1936–1942.
[33] R.J. Verma, Aflatoxin cause DNA damage, Int. J. Hum. Genet. 4 (2004) 231–236.
[34] H.N. Mishra, Chitrangada Das, A review on biological control and metabolism of aflatoxin, Crit. Rev. Food Sci. 43 (2003) 245–264.